Static Plate Load Test in Local Foundation Code – A Case Study

Arthur K O So

Meinhardt Infrastructure and Environment Limited (Email: arthurso@meinhardt.com.hk)
& AKOS Geotechnical Consulting Limited (Email: arthurkoso@hotmail.com)

doi: https://doi.org/10.21467/proceedings.7.7.30

ABSTRACT

Footings and raft foundations remain widely used in many countries. Local designs often rely on empirical formulae derived over fifty years ago. Prior to construction, a plate load test is required to verify the allowable bearing capacity of the supporting stratum, as stipulated in the Code of Practice for Foundations by the Buildings Department, first issued in 2004 and revised in 2017. Using a large raft foundation from a project as an example, the author proposes a more practical approach: reverting the test load to three times the working pressure, as specified in the 2004 Code, while increasing the allowable settlement by 2.5 mm to account for elasto-viscous deformation under higher loads. For very large raft foundations, the allowable bearing capacity should be capped, and the test may be eliminated entirely. Additionally, soil stiffness is not a material constant as the secant modulus varies with mean stress levels. As soil modulus degrades with increasing strain, the elastic modulus derived from load-settlement data tends to be stiffer than the design value used for settlement calculations at higher strains. The current approach to deducing operational soil stiffness for design purposes requires reconsideration.

1. INTRODUCTION

Footings and raft foundations remain widely used in many countries. Local design practices typically follow the Code of Practice for Foundations (BD, 2017), specifically Clause 2.2. It permits the determination of the allowable bearing capacity (q_a) either through presumed values in Table 2.1 of the 2017 Code or by rational design methods based on sound engineering principles for calculating the ultimate bearing capacity (q_u). Clause 2.2.4 suggests a bearing capacity equation derived from the work of Vesic (1973, 1975):

$$q_u = Q_u/B'L' = c'N_c\zeta_{cs}\zeta_{ci}\zeta_{cg}\zeta_{ct} + qN_q\zeta_{qs}\zeta_{qi}\zeta_{qg}\zeta_{qt}B'L' + 0.5B'\gamma_s'N_\gamma\zeta_{\gamma s}\zeta_{\gamma i}\zeta_{\gamma g}\zeta_{\gamma t} \quad (1)$$

where

N_c, N_γ, N_q	= general bearing capacity factors
Q_u	= ultimate resistance against bearing capacity failure which determine the capacity of a long strip footing
c'	= effective cohesion of soil
γ_s'	= effective unit weight of soil
q	= overburden pressure in the ground adjacent to the foundation and at same level as the base of the foundation
B	= least dimension of footing
L	= longer dimension of footing
B'	= B-e_B
L'	= L-$2e_L$
e_B	= eccentricity of load along B direction
e_L	= eccentricity of load along L direction
ζ_{cs}, ζ_{qs} $\zeta_{\gamma s}$	= influence factors for shape of foundation
ζ_{ci}, ζ_{qi}, $\zeta_{\gamma i}$	= influence factors for inclination of load
ζ_{cg}, ζ_{qg}, $\zeta_{\gamma g}$	= influence factors for ground surface
ζ_{ct}, ζ_{qt}, $\zeta_{\gamma t}$	= influence factors for tilting of foundation base

According to Clause 13 of the General Requirements for Foundation Works SE-SC1 (BD, 2020) and Section 17(1) of the Buildings Ordinance, engineers must verify the adequacy of the founding stratum's allowable bearing capacity through static plate load tests. The procedures and acceptance criteria for these tests are detailed

Proceedings DOI: 10.21467/proceedings.7.7; Series: AIJR Proceedings; ISSN: 2582-3922; ISBN: 978-81-989164-3-3

in Clause 8.2 of the Code of Practice for Foundations (BD, 2004 and revised in 2017). However, recent research suggests that the q_u calculated using Equation [1] may be overestimated for large rafts. Furthermore, the test procedures outlined in the 2017 Code may not adequately verify the founding stratum's suitability. For instance, the elastic modulus E back-calculated from load-settlement data often differs from the design values used in settlement calculations.

2. THE BEARING CAPACITY EQUATION

The analysis of ultimate loads for shallow foundations dates back nearly 170 years. Early work on the subject was initiated by Rankine (1857), followed by Prandtl (1920) who studied the plastic deformation of metals. Caquot (1934) first applied plasticity theory to foundation analysis. Buisman (1940) extended this to soils with weight, introducing the superposition of the weight term (N_γ) with the cohesion (N_c) and surcharge (N_q) terms in the bearing capacity equation. Terzaghi (1943) identified three principal modes of bearing capacity failure and proposed the basic equation $q_u = cN_c + qN_q + ½\gamma BN_\gamma$. Meyerhof (1963) expanded on these ideas and derived practical formulae for designing both rigid and flexible foundations. Hansen (1970) proposed a general bearing capacity equation to account for footings on sloping ground or with tilted bases. Vesic (1973) refined Hansen's equation and derived Equation [1]. The equations developed by Meyerhof, Hansen, and Vesic remain widely used today.

The Bearing Capacity Factors N_c, N_q, and N_γ

Over the years, numerous correction factors for N_c, N_q and N_γ have been proposed. These factors are typically semi-empirical and account for specific effects by multiplying the three terms in the bearing capacity equation. Analytical methods include: the limit equilibrium techniques (Terzaghi, 1943; Meyerhof, 1951), the slip-line methods (Sokolovski, 1960), the limit analysis methods (Chen and Davidson, 1973), and the finite element methods (Griffith, 1982). Experimental methods, such as laboratory tests (Schanz and Vermeer, 1996), full-scale in-situ tests (Briaud and Gibbens, 1994), and centrifuge tests (Okamura et al., 2002), have also been employed. However, these methods have limitations. For example, model footings suffer from scale effects, while full-scale tests are costly and time-consuming. Centrifuge testing, though promising, has not gained widespread adoption due to challenges in accurately simulating soil behaviour.

Okamura et al. (2002) identified three key factors that reduce bearing capacity: the loading conditions, scale effects and footing shape effects. Nguyen et al. (2016) noted that most bearing capacity equations are limited to simple footing shapes and uniform ground conditions, neglecting scale effects. Taghvamanesh and Moayed (2021) reviewed 60 models and found that while N_c and N_q are well-correlated and straightforward to compute, N_γ values vary widely. They attributed this discrepancy to differences in assumptions about the soil wedge beneath the footing (Das, 2004) and the computation of passive earth pressure (Zhu et al., 2001). They concluded that N_γ depends not only on the friction angle (ϕ) but also on footing width (B), dilatation angle (ψ), and relative density (D_r). Specifically, N_γ decreases as B and D_r increase, highlighting the importance of scale and shape effects.

The Scale Effect

Equation [1] suggests that $q_u = ½\gamma BN_\gamma$ when c is zero and q is negligible. This implies that q_u increases linearly with BN_γ or B, which is unrealistic if N_γ depends solely on ϕ. De Beer (1965) was among the first to recognize the scale effect, reporting that the strength envelope in triaxial tests on sand is non-linear and characterized by a secant ϕ that increases with D_r. Vesic (1973) attributed the decrease in strength with foundation size to the curvature of the Mohr envelope, progressive rupture along slip lines, and presence of weak zones or seams in soil deposits. Habib (1974) introduced a modified bearing capacity factor $N^*_\gamma = N_\gamma + 400/n$ where $n = B/\delta$ (with δ being the mean grain size in mm). The Architectural Institute of Japan (AIJ, 1988 and 2001) proposed a modified equation incorporating shape coefficients (α, β) and a scale factor (η). Shiraishi (1990) suggested $N^*_\gamma = 0.71N_\gamma/B^{0.2}$ while Bowles (1997) recommended a reduction factor $r_\gamma = 1 - 0.25\log(B/\kappa)$ where $B \geq 2$m and $\kappa = 2.0$. Ueno et al. (1998) highlighted the stress level effect on shear strength, noting that mean stress beneath foundations ranges from $2\gamma B$ to $10\gamma B$, affecting the internal friction angle. Cerato and Lutenegger (2006) demonstrated that N_γ decreases with B and increases with D_r, with D_r having a more pronounced influence than δ. Lau and Bolton (2011a, 2011b) introduced a variable ϕ analysis, showing that secant ϕ varies linearly with the logarithm of mean effective stress in granular soils.

The Shape Effect

For non-rectangular foundation shapes, obtaining analytical solutions is challenging. Engineers have relied on semi-empirical methods, often based on comparative loading tests with footings of different shapes. These tests show that shape factors depend primarily on ϕ and other parameters, often expressed as constants or simple functions of foundation geometry (B and L). Some examples are given in Table 1. This implies that shape and scale effects are interrelated.

Table 1 – Shape Factors Proposed by Various Authors and the Calculated q_u

Authors	ζ_{cs}	ζ_{qs}	$\zeta_{\gamma s}$	q_u (kPa)
Myerhoff (1963)	1+0.2K_p(B/L) for any ϕ K_p = tan^2(45°+ϕ/2)	1 for ϕ = 0° 1+0.1K_p(B/L) for ϕ > 10° K_p = tan^2(45°+ϕ/2)	1 for ϕ = 0° 1+0.1K_p(B/L) for ϕ > 10° K_p = tan^2(45°+ϕ/2)	2,507
Hansen (1970)	0.2(B/L) for ϕ = 0° 1+(N_q/N_c)(B/L) for $\phi \neq$ 0°	1+(B/L)tanϕ	1-0.4(B/L) ≥ 0.6	1,381
Vesic (1973)	1+(N_q/N_c)(B/L)	1+(B/L)tanϕ	1-0.4(B/L) ≥ 0.6	1,381
Perau (1997)	-	1+1.6tanϕ(B/L)[1+(B/L)^2]	1 / [1+(B/L)]	1,128
Zhu and Michalowski (2005)	-	-	1+(0.6sin$^2\phi$-0.25(B_f/L_f) for ϕ ≤ 30° 1+(1.3sin$^2\phi$-0.5(L_f/B_f)$^{1.5}$exp(-L_f/B_f)) for ϕ > 30°	2,308
EN7 (2005)	1+0.2K_p(B/L) for ϕ = 0 ζ_{cs} (N_q-1)/(N_q-1) for $\phi \neq$ 0°	1+(B/L)sinϕ	1-0.3(B/L)	1,532

The Elastic Modulus of Soil

According to Lau and Bolton (2011a), the secant ϕ is not a material constant for granular soils but is highly sensitive to the mean stress level. The vertical stress in the supporting soil ranges from the bearing capacity (q_u) directly underneath the footing to the overburden pressure (q) at the edge. The contact pressure distribution under the footing is also highly non-uniform. Consequently, stress variations cause the mobilized angle of friction (ϕ_m) to vary significantly from point to point. Bolton (1986) attributed this variation in secant ϕ to the strength dilatancy of sands and the crushing of particles at the high end of the stress range. A factor of 50 in confining stress would result in a factor of about 7 in the stiffness of granular soils.

Summary

This literature review has outlined the derivation and limitations of Equation [1], alongside recent findings on scale and shape effects in raft foundation design. Following the implementation of the 2017 Code, feedback from engineers and practitioners has highlighted several practical challenges and concerns. To further explore these issues, the following sections will examine a case study involving the design of a raft foundation from a real-world project. This case study will illustrate key observations related to the 2017 Code and provide actionable recommendations for improvement.

3. THE RAFT FOUNDATION DESIGN

The project involves the design and construction of a 2-storey building with a green roof, as depicted in Figure 1, along with an annex building located nearby. Borehole data reveals that the geology beneath the 2-storey building consists of varying thicknesses of fill, colluvium, alluvium, and completely decomposed granite (CDG) to highly decomposed granite (HDG), followed by rock (Figure 1(b)). Given the relatively low design loading, a shallow raft foundation appears to be the most suitable option. An alternative option, such as large-diameter bored piles on Category 1(d) rock, was considered but deemed less favorable due to the uncertainty in the depth of Category 1(d) rockhead. Driven H-piles were ruled out due to the potential vibration impact on nearby Mass Transit Railway tunnels.

A 0.8-meter-thick leveled raft foundation resting on CDG was designed. The design parameters are summarized in Table 2. The raft is assumed to be rigid, while the CDG is modeled as perfectly elastic-plastic in the analysis. The allowable settlement (S_a) for the project is 30.0 mm. Using the software SAFE, the maximum bearing pressure (q_{max}) of the raft foundation was determined to be 383 kPa at the edge (Figure 1(c)). Assuming E = 1.5N where N is the number of blows in standard penetration test, the maximum settlement (S_{max}) was calculated as 26.2 mm using Schmertmann's (1970) method, as recommended in GEO Publication No. 1/2006 (GEO, 2006). Since the raft foundation is irregularly shaped, the calculation of B and L is based on the largest inscribed rectangle, as per Note (6) of the Clause and Figure 2.4 in the 2017 Code. Thus, B = 14.6 m and L = 19.2 m were adopted, with e_B and e_L ignored (Figure 1(d)). The calculated q_u was applied to the entire raft. Using equation [1], q_u and the q_a were determined to be 1,381 kPa and 460 kPa, respectively, ignoring the 0.8 m overburden. Since q_a > q_{max} (383 kPa), the design is deemed acceptable.

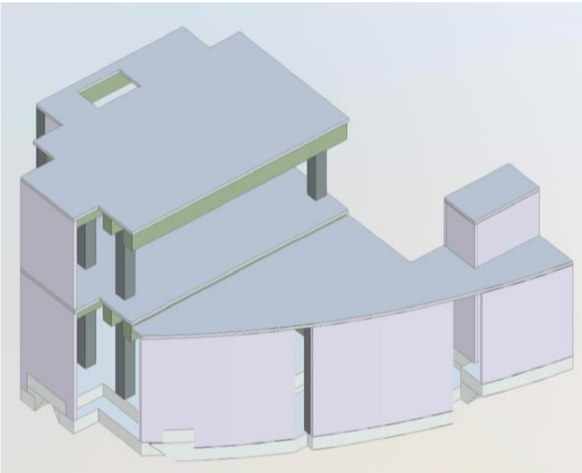

(a) Pictorial View of the Sports Building

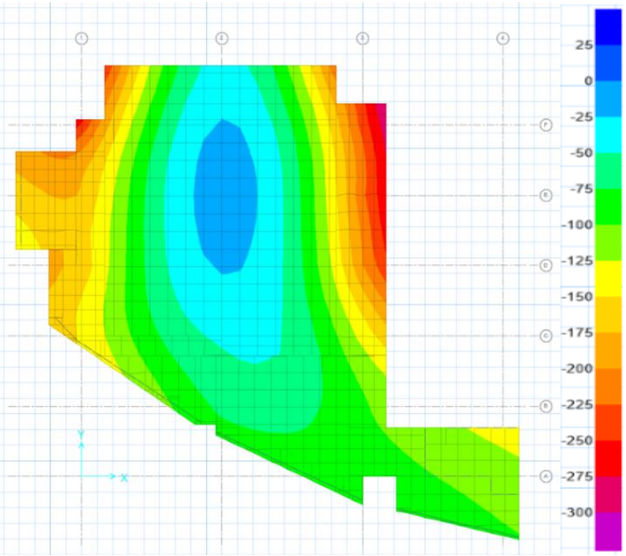

(c) Pressure Distribution (kPa)

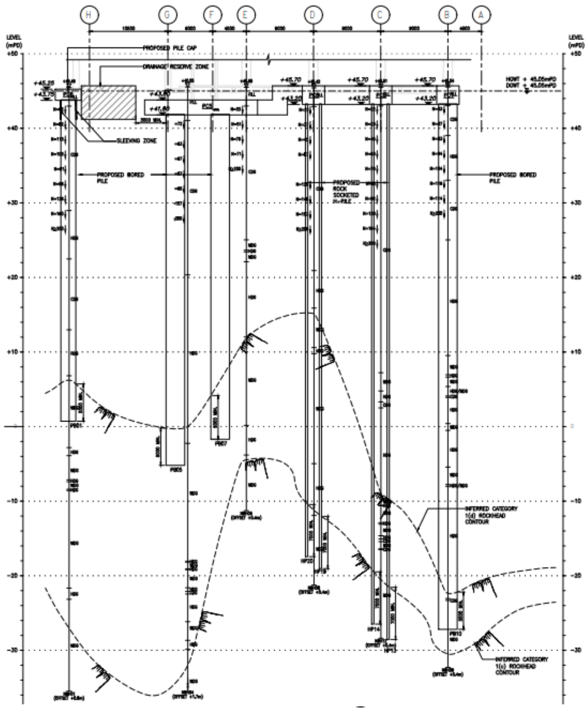

(b) Geological Profile along the Sports Building

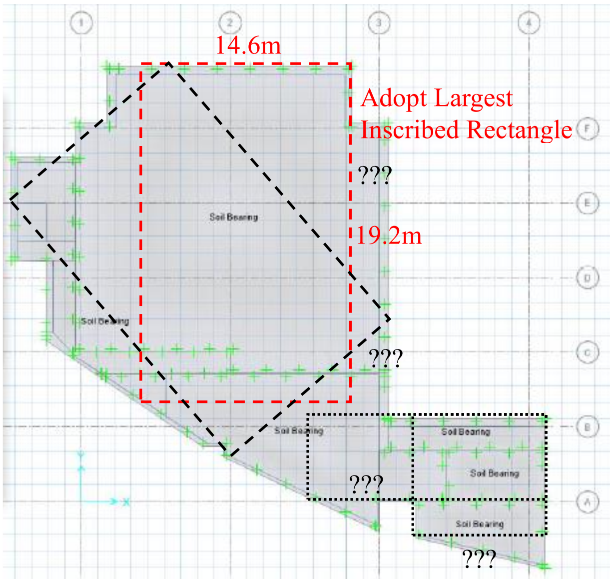

(d) Determination of Largest Inscribed Rectangle

Figure 1 – General View, Geology and Soil Pressure Distribution of the Building Structure

Table 2 – Design Parameters for the Raft Foundation

Design Parameters	Values
Existing Ground Level (mPD)	+45.7
Design Ground Water Level (mPD)	+45.7
Formation Level (mPD)	+44.9
Design Vertical Load (kN)	33,348
Design Horizontal Load (kN)	218
Eccentricity of Load along Least Dimension e_B (m)	4.02
Eccentricity of Load along Longer Dimension e_L (m)	4.33
Friction Angle ϕ' of CDG (degree)	32
Cohesion of c' of CDG (kPa)	0
Bulk Density of CDG (kN/m^3)	19
Poisson Ratio ν of CDG	0.3

4. THE PLATE LOAD TEST PROCEDURES AND ACCEPTANCE CRITERIA

According to Clause 8.2 of the 2004 Code, the maximum test load (proof load) shall be $3W$, where W is the allowable working pressure multiplied by the area of the loading plate: 3×383 kPa $\times \pi \times 0.15$ m² = 81.22 kN. This implies that the maximum test pressure under the loading plate is $3q_{max} = 3 \times 383$ kPa = 1,149 kPa, which is less than q_u (1,381 kPa) as determined by the bearing capacity equation [1]. The acceptance criteria specify that S_{max} shall not exceed S_p, calculated as: $S_p = 3\ S_f \times [(B + b) / 2B]^2 \times (m + 0.5) / (1.5m)$, where S_f = allowable settlement of the footing under the allowable working load, b = diameter or least dimension of the plate, and m = length-to-width ratio of the footing ($m \geq 1$). For m = 19.2 m / 14.6 m = 1.3, S_p is calculated as: 3 × 30 mm × [(14.6m+0.3m)/(2×14.6m)]^2 ×(1.3+0.5)/(1.5×1.3) = 21.6mm.

However, the 2017 Code revised the proof load to $\geq 3W_t$, where W_t = ⅓ $(q_u)_{plate}$ x A_{plate}. Here, $(q_u)_{plate}$ = ultimate bearing capacity of the test plate based on N_c and N_γ, and A_{plate} = area of the test plate. As explained in Clause H8.2(A) of the Explanatory Handbook to the Code (HKIE, 2017), N_q is ignored because no adjacent surcharge is applied during the plate load test. For CDG, c' = 0 kPa and N_c = 0. Equation [1] simplifies to: $(q_u)_{plate} = 0.5B'\gamma_s' N_\gamma \zeta_{\gamma s} \zeta_{\gamma i} \zeta_{\gamma g} \zeta_{\gamma t}$ = 0.5 × 0.3 m × 19 kN/m³ × 30.2 × 0.6 × 1 × 1 × 1 = 52 kPa. The proof load is calculated as: 3 × ⅓ ×52 kPa × π × 0.5 m² = 3.65 kN. The acceptance criteria specify that S_{max} shall not exceed $S_p = 0.15B$ = 0.15 × 300 mm = 45.0 mm. The above calculations are summarized in Table 3. While the designed q_{max} of the raft foundation is 383 kPa, the bearing soil is required to be tested to 1,149 kPa (or 81.22 kN) under the 2004 Code but only to 52 kPa (or 3.65 kN) under the 2017 Code. At the same time, the acceptable S_p increases from 21.6 mm to 45.0 mm. This discrepancy warrants further investigation.

Table 3 – Summary of Design Calculations

	Design Model	Bearing Capacity Equation	Plate Load Test BD (2004)	Plate Load Test BD (2017)
Bearing Pressure	q_{max} = 383kPa	q_u = 1,381kPa q_a = 460kPa	Testing plate pressure = 3*q_{max} =1,149kPa	Testing plate pressure = $(q_u)_{plate}$ = 52kPa
Test Load	-	-	$3W$ = 81.22kN	$3W_t$ = 3.65kN
Settlement	S_{max} = 26.2mm	-	Allowable S_p = 21.6mm	Allowable S_p = 45.0mm

5. OBSERVATIONS AND DISCUSSIONS

The Scale Effect

Figure 2 illustrates the variation of q_u with B, keeping the B/L ratio constant at 0.76 (= 14.6 m / 19.2 m). Assuming no eccentric load for simplicity, and using a mean grain size of 0.1 mm in the Habib (1974) equation and B_0 = 5 m in the AIJ (1988, 2001) equation, the following observations were made: The Habib (1974) prediction closely aligns with Vesic's (1973) results and is insensitive to the mean grain size. The AIJ (1988, 2001), Shiraishi (1990), and Bowles (1997) predictions show an increase in q_u with B, but the rate of increase diminishes as B grows, highlighting the significance of the scale effect for large footings. For the raft foundation in this project, q_u was calculated as 1,381 kPa using equation [1] without considering the scale effect. However, when the scale effect is considered, q_u reduces to 958 kPa (69%), 574 kPa (42%), and 1,079 kPa (78%) based on the AIJ (1988, 2001), Shiraishi (1990), and Bowles (1997) methods, respectively. Consequently, the q_a varies from 193 kPa (= 460 kPa × 42%) to 359 kPa (= 460 kPa × 78%), which is less than the designed q_{max} = 383 kPa. This finding aligns with Table 2.1 in the 2004 and 2017 Codes, which specify presumed allowable vertical bearing pressures of 250 kPa for very dense non-cohesive soil (SPT > 50) and 1,000 kPa for intermediate soil (SPT ≥ 200).

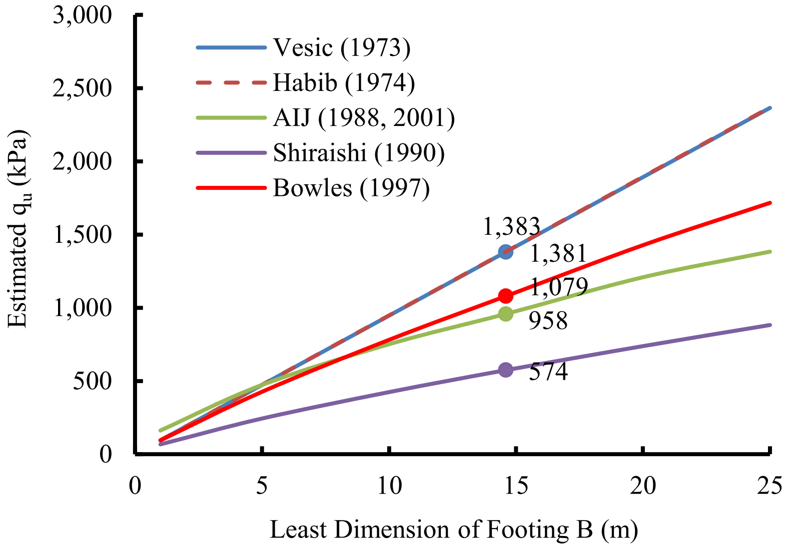

Figure 2 – Variation of q_u with B

The Shape Effect

For irregularly shaped raft foundations, the calculation of B and L in the Code is based on the largest inscribed rectangle. However, several questions arise: Is the largest inscribed rectangle determined by area or perimeter (see Figure 1(c))? Should eccentricities e_B and e_L be ignored or calculated from the largest inscribed rectangle? Should the calculated q_u be applied to the entire raft, or should other areas be ignored? If not, should the raft be divided into multiple rectangles, each with its own q_u? These questions highlight that the calculation of B and L is more of an art than a science, relying heavily on experience and interpretation.

Figure 3 demonstrates the shape effect on q_u. Keeping B constant at 14.6 m, Meyerhoff (1963) suggests an increase in q_u as B/L increases, while Zhu and Michalowski (2005) indicate a decrease in q_u as B/L increases, with a minimum q_u at B/L = 0.6 and a slight increase for B/L > 0.6. Other researchers, including Hansen (1970), Vesic (1973), Perau (1997) and EN7 (2005), show a decrease in q_u as B/L increases. For the raft foundation in this project, q_u ranges from 1,128 kPa to 2,507 kPa for B/L = 0.76, based on shape factors proposed by various authors. However, these values could change if the shape of the raft changes, underscoring the importance of accurately determining the largest inscribed rectangle as per the 2017 Code.

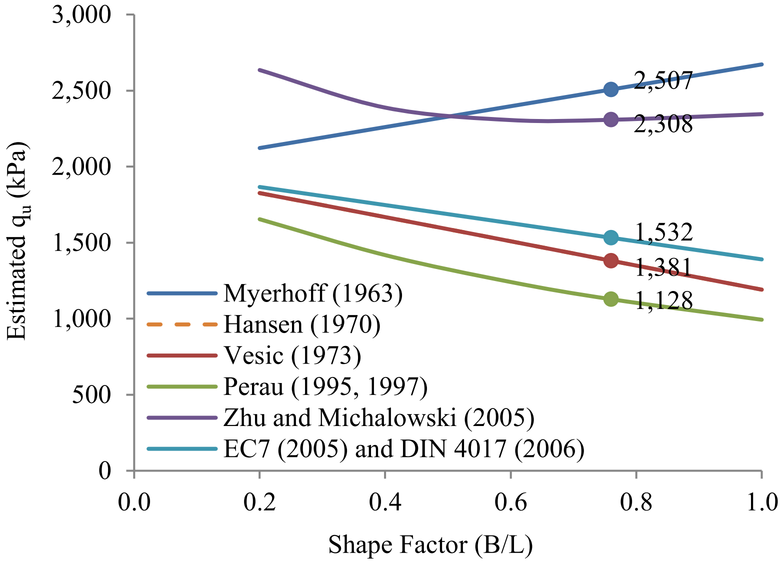

Figure 3 – Effect of Shape Factor on q_u

The Static Plate Load Test

The limitations of the plate load test are discussed in Clause H8.2 of the Explanatory Handbook to the Code of Practice for Foundations (HKIE, 2014 and 2017) and Clause 3.4 of GEO Publication No. 1/2006 (GEO, 2006). According to Clause 8.2(1) of the 2017 Code, the static plate load test is intended to verify q_a and E used in settlement calculations through back-analysis. Figure 4 overlays the test loads and allowable S_p with the typical stress-strain curve of a cohesionless soil. In the 2004 Code, the test load is three times the working pressure $3W$ (1,149 kPa), placing it in the non-linear portion of the stress-strain curve. Since soil is typically modeled as elasto-plastic in design, it is unsurprising that the anticipated S_p may exceed the allowable S_p when the test load approaches q_u (1,381 kPa). In contrast, the 2017 Code reduces the test load to three times the ultimate bearing capacity of the test plate $3W_t$ based on N_c and N_γ only, resulting in a much smaller load (52 kPa, or 4.5% of the value in 2004 Code). This load falls in the early linear portion of the stress-strain curve, yet the permitted S_p increases from 21.6 mm to 45.0 mm, which is counterintuitive. As a result, the test to verify the adequacy of the founding stratum's allowable bearing capacity under the 2017 Code may not be meaningful.

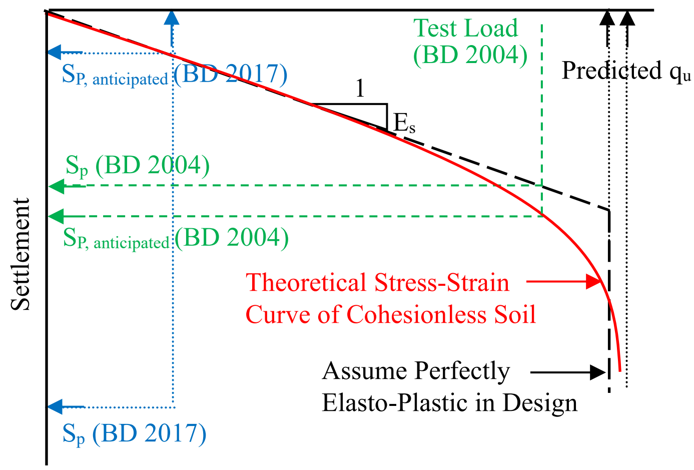

Figure 4 – Schematic Representation of the Static Plate Load Test (Not to Scale)

The Back-Calculated Elastic Modulus

Figure 5(a) illustrates the determination of the elastic modulus or stiffness of soil. In theory, it is equal to the slope of the stress-strain line. If this stress-strain line is linear, the slope is easily determined as the ratio of the

Proceedings DOI: 10.21467/proceedings.7.7
ISBN: 978-81-989164-3-3

Series: AIJR Proceedings
ISSN: 2582-3922

stress along an axis to the strain along that axis within the range of elastic soil behavior, and is shown as the initial tangent modulus. However, when the soil behavior becomes non-linear, the gradient of the stress-strain line decreases progressively. The gradient at that point, known as the tangent modulus, represents the soil stiffness at a specific stress level σ. If one connects the end points of the stress-strain diagram at the point of interest with a straight line, the slope of that straight line is the secant modulus, which is traditionally used to back-calculate the soil modulus in the 2017 Code. As shown in Figure 5(b), soil is not a perfectly elastic-plastic material, and the secant modulus determined will therefore decrease as the strain increases. Since the test load in the 2017 Code is very small and should be in the early linear portion of the stress-strain curve, the elastic modulus back-calculated from the load-settlement behavior should be close to the $E_{initial}$. This value is stiffer than the design value at larger strains due to the degradation of the elastic modulus, and the settlement calculation will therefore be underestimated.

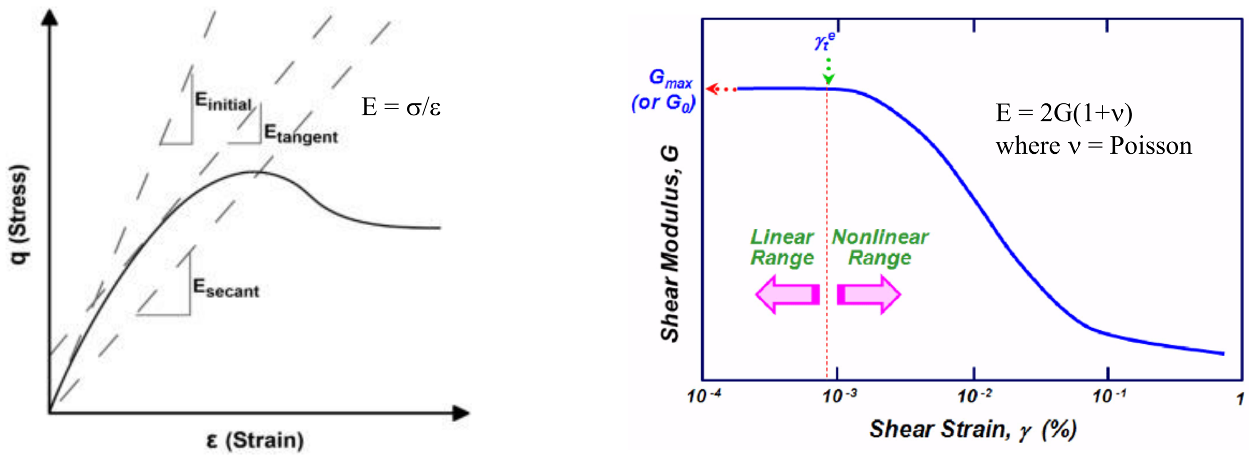

(a) Determination of Elastic Modulus (b) Degradation of Modulus

Figure 5 - Non-Linear Stress-Strain Characteristics of Soil

6. CONCLUSIONS AND RECOMMENDATIONS

The static plate load test is essential for verifying the adequacy of the founding stratum and back-calculating the soil's elastic modulus (E) from load-settlement behavior for settlement analysis. The 2017 Code bases the test load on the working pressure of the test plate, accounting for plate-scale capacity, whereas the 2004 criteria risk overloading the plate due to its requirement of three times the working pressure. Incorporating the plate-size dependent factors could better capture the observed non-linear soil behavior and size effects. However, the discrepancies between the 2004 and 2017 Codes raise concerns about test validity and interpretation.

In the 2004 Code, the test load is set at three times the working pressure, which is often high enough to place the soil in the non-linear portion of its stress-strain curve. Since soil is typically modeled as elasto-plastic for simplicity in design, the anticipated settlement (S_{max}) may exceed the permitted limits (S_p), particularly when the test load approaches the ultimate bearing capacity (q_u). Conversely, the 2017 Code specifies a test load of three times the ultimate bearing capacity of the test plate, derived solely from the bearing capacity factors (N_c and N_γ). This load is often too small, keeping the soil in the linear elastic range, while the permitted settlement (S_p) is significantly larger than that in the 2004 Code. As a result, the test may fail to meaningfully verify the allowable bearing capacity, as the outcomes are almost always deemed acceptable. A more balanced approach is to revert the test load to 3 times the working pressure, but the allowable S_{max} is revised to $\leq S_p = 3S_f \times [(B+b)/2B]^2 \times (m+0.5)/(1.5m) + \delta$. This adjustment δ is not for the purpose to reconcile differences in influence depth, but is the degree of mobilization to cater for the elasto-viscous behavior at large load. For simplicity, δ can be specified as a settlement limit equal to the quake which is the static relative movement between pile and soil that is required to mobilize the plastic resistance. Literature reviews by Soares et al. (1984) indicated that quake equal to 2.5mm is widely used. Larger value can be adopted for larger acceptable viscous behavior. For a very large raft foundation, the allowable bearing capacity should be capped based on local test data and the test can be removed entirely.

Soil stiffness is not a material constant, as the secant modulus (ϕ) varies with mean stress. Due to modulus degradation, the elastic modulus back-calculated from the load-settlement data tends to be stiffer than the design value at larger strains. Thus, the conventional approach to deriving an operational soil stiffness requires reconsideration. Improved estimation methods such as stress-dependent models or advanced testing (e.g., pressuremeter or seismic tests) could be adopted to better reflect design conditions.

In summary, clearer guidelines or alternative methods for calculating B and L should be provided, potentially using probabilistic approaches or case studies to reduce ambiguity. Future research should prioritize large-scale field tests to validate the bearing capacity and settlement predictions, investigate the B/L versus q_u relationship and δ across different soils and loading conditions, and develop standardized methods for estimating soil stiffness under varying stress levels. These advancements would lead to more reliable and efficient raft foundation design practices.

ACKNOWLEDGEMENT

I would also like to express my gratitude to The MTR Corporation Limited for the permission to use some raw design data taken from a project.

REFERENCES

AIJ, 1988, 2001. Recommendations for design of building foundations. *Architectural Institution of Japan*.

BD. 2004, 2017. Code of practice for foundations. *Buildings Department, The Government of the HKSAR.*

BD. 2020. The general requirements for foundation Works – SE-SC1 (9/2020). The Common Conditions and Requirements, *Buildings Department, The Government of the HKSAR.*

Bolton, M. D. 1986. The strength and dilatancy of sands. *Geotechnique*, 36(1), pp. 65-78.

Bowles, J. E. 1997. *Foundation analysis and design*. McGraw-Hill, 5th Edition, McGraw Hill, Singapore.

Briaud, J. L. and Gibbens, R. (1994). Test and prediction results for five large spread footings on sand. *ASCE Geotechnical Special Publication 41, Predicted and Measured Behavior of Five Spread Footings on Sand*, Briaud J L and Gibbens R (Eds) ASCE, New York, pp. 92-128.

Buisman, A. S. K. 1940. *Grondmechanica*. Waltman, Delft, The Netherlands.

Caquot. A. 1934. *Equilibrium des Massifs a frottement Interne*. Gauthier-Villars, Paris, France, pp. 1-91.

Cerato, A. B. and Lutenegger, A. J. 2006. Scale effects of shallow foundation bearing capacity on granular material. *BGA International Conference*.

Chen, W. F. and Davidson, H. L. 1973. Bearing capacity determination by limit analysis. *Journal of the Soil Mechanics and Foundations Division, ASCE* 99(6), pp. 433-449.

Das, B. M. 2004. *Soil Mechanics.* The Engineering Handbook, Second Edition, pp. 81-1 to 81-7.

De Beer, E. E. 1965. The scale effect on the phenomenon of progressive rupture in cohesionless soils. *Proceedings, Sixth International Conference on Soil Mechanics and Foundation Engineering,* Montreal, Canada, 2, pp. 13-17.

De Beer, E E 1970. Experimental determination of the shape factors and the ultimate bearing capacity factors of sand. *Geotechnique,* 20(4), pp. 387-411.

EN7. 1997. *Geotechnical design – Part 1: General rules.* BS EN 1997-1:2004, Eurocode 7.

GEO. 2006. *Foundation Design and Construction. GEO Publication No. 1/2006,* Geotechnical Engineering Office, Civil Engineering and Development Department, The Government of the HKSAR.

Griffith, D. V. 1982. Computation of bearing capacity factors using finite elements. *Geotechnique,* (32)3, pp. 195-202.

Habib, P. A. 1974. Scale effect for shallow footings on dense sand. *Journal of the Geotechnical Engineering Division, ASCE,* 100(GT1), pp. 95-99.

Hansen, J. B. 1970. A revised and extended formula for bearing capacity. *Bulletin of Danish Feotechnical Insitute*, 8, pp. 5-11.

HKIE. 2014, 2017. *An explanatory handbook to the code of practice for foundations*. The Hong Kong Institution of Engineers, The Government of the HKSAR.

Lau, C. K. and Bolton, M. D. 2011a. The bearing capacity of footings on granular soils. I: Numerical analysis. *Geotechnique,* 61(8), pp. 627-638.

Lau, C. K. and Bolton, M. D. 2011b. The bearing capacity of footings on granular soils. II: Experimental evidence. *Geotechnique,* 61(8), pp. 639-650.

Meyerhof, G. G. 1951. The ultimate bearing capacity of foundations. *Geotechnique,* 1(2), pp. 301-332.

Meyerhof, G. G. 1963. Some recent research on the bearing capacity of foundations. *Canadian Geotechnical Journal,* 1, pp. 16-26.

Nguyen, D. L., Ohtsuka, S., Hoshina, T. and Isobe, K. 2016. Discussion on size effect of footing in ultimate bearing capacity of sandy soil using rigid plastic finite element method. *Soils and Foundations, Japanese Geotechnical Society,* 56(1), pp. 93-103.

Okamura, M., Mihara, A., Takemura, J. and Kuwano, J. 2022. Effects of footing size and aspect ratio on the bearing capacity of sand subjected to eccentric loading. *Soils and Foundations, Japanese Geotechnical Society,* 42(4), pp. 43-56.

Perau, E. W. 1997. Bearing capacity of shallow foundations. *Soils and Foundations, Japanese Geotechnical Society,* 37(4), pp. 77-83.

Prandtl, L. 1920. Uber die Eindringungsfestigkeit (Harte) Plastischer Baustoffe und die Festigkeit von Schneiden. *Zeitschrift fur Angewandte Mathematik und Mechanik*, Berlin, 1(1), pp. 15-20.

Rankine, W. 1857. On the stability of loose earth. *Philosophical Transactions of the Royal Society of London*, 147.

Schanz, T. and Vermeer, P. A. 1996. Angles of friction and dilatancy of sand. *Geotechnique*, 46(1), pp. 145-151.

Schmertmann, J. 1970. Static cone to compute static settlement over sand. *Journal of Soil Mechanics and Foundation Division, ASCE*, 96, pp. 1011-1043.

Shiraishi, S. 1990. Variation in bearing capacity factors of dense sand assessed by model loading tests. *Soils and Foundations, Japanese Geotechnical Society*, 30(1), pp. 17-26.

Soares, M. M., Matos, S. F. D. and de Mello, J. R. C. 1984. Pile driveability studies, pile driving measurements. *Proceedings of the Second International Conference on the Applications of Stress-Wave Theory of Piles, Stockholm*, pp. 64-71.

Sokolovski, V. V. 1960. *Statics of soil media*. Butterworth Scientific Publications, London, UK.

Taghvamanesh, S. and Moayed, R. Z. 2021. A review on bearing capacity factor N_γ of shallow foundations with different shapes. *World Academy of Science, Engineering and Technology, International Journal of Geotechnical and Geological Engineering*, 15(8).

Terzaghi, K. 1943. *Theoretical soil mechanics*. 5th Edition, John Wiley and Sons Inc., New York.

Ueno, K., Miura, K. and Maeda, Y. 1998. Prediction of ultimate bearing capacity of surface footings with regard to size effects. *Soils and Foundations, Japanese Geotechnical Society*, 38(3), pp. 165-178.

Vesic, A. S. 1973. Analysis of ultimate loads of shallow foundations. *Journal of the Soil Mechanics and Foundations Division, ASCE*, 99(1), pp. 45-73.

Vesic, A. S. 1975. *Bearing capacity of shallow foundations. Foundation Engineering Handbook*, Edited by Winterkorn, H.F. and Fang, H.Y., Van Nostrand Reinhold, New York, pp. 121-147.

Zhu, D. Y., Lee, C. F. and Jiang, H. D. 2001. A numerical study of the bearing capacity factor N_γ. *Canadian Geotechnical Journal*, 38(5), pp. 1090-1096.

Zhu, M. and Michalowski, R. L. 2005. Bearing capacity of rectangular footings on two-layer clay. *Proceeding of the 16th International Conference on Soil mechanics and Geotechnical Engineering, Osaka*, pp. 997-1000.